



Evidence for Right Ventricular Lipotoxicity in Heritable Pulmonary Arterial Hypertension

Anna R. Hemnes¹, Evan L. Brittain², Aaron W. Trammell¹, Joshua P. Fessel¹, Eric D. Austin³, Niki Penner¹, Karen B. Maynard¹, Linda Gleaves¹, Megha Talati¹, Tarek Absi⁴, Thomas DiSalvo², and James West¹

¹Division of Pulmonary and Critical Care Medicine, ²Division of Cardiovascular Medicine, ³Division of Allergy, Immunology, and Pulmonary Medicine, Department of Pediatrics, and ⁴Department of Cardiac Surgery, Vanderbilt University Medical Center, Nashville, Tennessee

Abstract

Rationale: Shorter survival in heritable pulmonary arterial hypertension (HPAH), often due to *BMPT2* mutation, has been described in association with impaired right ventricle (RV) compensation. HPAH animal models are insulin resistant, and cells with *BMPT2* mutation have impaired fatty acid oxidation, but whether these findings affect the RV in HPAH is unknown.

Objectives: To test the hypothesis that *BMPT2* mutation impairs RV hypertrophic responses in association with lipid deposition.

Methods: RV hypertrophy was assessed in two models of mutant *Bmpr2* expression, smooth muscle-specific (*Sm22*^{R899X}) and universal expression (*Rosa26*^{R899X}). Littermate control mice underwent the same stress using pulmonary artery banding (Low-PAB). Lipid content was assessed in rodent and human HPAH RVs and in *Rosa26*^{R899X} mice after metformin administration. RV microarrays were performed using human HPAH and control subjects.

Results: RV/(left ventricle + septum) did not rise directly in proportion to RV systolic pressure in *Rosa26*^{R899X} but did in *Sm22*^{R899X} ($P < 0.05$). *Rosa26*^{R899X} RVs demonstrated intracardiomyocyte triglyceride deposition not present in Low-PAB ($P < 0.05$). RV lipid deposition was identified in human HPAH RVs but not in controls. Microarray analysis demonstrated defects in fatty acid oxidation in human HPAH RVs. Metformin in *Rosa26*^{R899X} mice resulted in reduced RV lipid deposition.

Conclusions: These data demonstrate that *Bmpr2* mutation affects RV stress responses in a transgenic rodent model. Impaired RV hypertrophy and triglyceride and ceramide deposition are present as a function of RV mutant *Bmpr2* in mice; fatty acid oxidation impairment in human HPAH RVs may underlie this finding. Further study of how *BMPT2* mediates RV lipotoxicity is warranted.

Keywords: heart failure; pulmonary hypertension; right ventricle; insulin resistance

Although pulmonary arterial hypertension (PAH) is a highly morbid disease of the pulmonary vasculature with progressive arterial obliteration, the resultant cause of death in this condition is right heart failure (1). Recent large-scale registries of patients

with PAH have shed light on important subtypes of disease that are associated with increased mortality (2, 3). Data from the Registry to Evaluate Early and Long-Term PAH Disease Management (REVEAL) registry demonstrated greater than twofold

increased hazard ratio for mortality among patients with heritable PAH compared with patients with idiopathic PAH (3), and we and others have shown depressed right ventricular stroke work index and cardiac index in heritable PAH (4, 5), suggesting

(Received in original form June 14, 2013; accepted in final form November 12, 2013)

Supported by National Institutes of Health grants K08 HL093363 and 1P01HL108800 (A.R.H.), R01s HL82694 and HL95797 (J.W.), K23 HL0987431 (E.D.A.), and T32 HL094296 (J.P.F.). The Mouse Metabolic Phenotyping Core (MMPC) is supported in part by grant U24 DK059637.

Author Contributions: A.R.H. designed studies, analyzed data, and prepared and reviewed the manuscript. E.L.B. designed studies, analyzed data, and reviewed the manuscript. A.W.T. designed studies, analyzed data, and reviewed the manuscript. J.P.F. designed studies, analyzed data, and reviewed the manuscript. E.D.A. designed studies, analyzed data, and reviewed the manuscript. N.P. performed experiments and analyzed data. K.B.M. performed experiments and analyzed data. L.G. performed experiments, designed studies, and analyzed data. M.T. designed studies, analyzed data, and reviewed the manuscript. T.A. collected data and reviewed the manuscript. T.D. analyzed data and reviewed the manuscript. J.W. designed studies, analyzed data, and reviewed the manuscript.

Correspondence and requests for reprints should be addressed to Anna R. Hemnes, M.D., Division of Pulmonary and Critical Care Medicine, Vanderbilt University Medical Center, T1218 Medical Center North, 1161 21st Avenue South, Nashville, TN 37232. E-mail: anna.r.hemnes@vanderbilt.edu

This article has an online supplement, which is accessible from this issue's table of contents at www.atsjournals.org

Am J Respir Crit Care Med Vol 189, Iss 3, pp 325–334, Feb 1, 2014

Copyright © 2014 by the American Thoracic Society

Originally Published in Press as DOI: 10.1164/rccm.201306-1086OC on November 25, 2013

Internet address: www.atsjournals.org

At a Glance Commentary

Scientific Knowledge on the Subject:

Increased glycolysis and decreased fatty acid oxidation have been reported in right ventricular failure associated with rodent models of pulmonary arterial hypertension (PAH). The consequences of impaired fatty acid oxidation have not been explored.

What This Study Adds to the Field:

Our research shows that expression of genes from the fatty acid oxidation pathway is suppressed in failing right ventricles (RVs) from patients with PAH and that cardiomyocyte lipid deposition is present in the same RVs. We found RV lipid deposition in a transgenic rodent model of PAH using universal expression of mutant *BMPR2*, a gene that commonly underlies heritable PAH. In a rodent model, we characterized the lipid as triglyceride and found that compensatory RV hypertrophy is reduced when *BMPR2* is expressed in the RV. These findings suggest impaired fatty acid oxidation is associated with lipid deposition in the RV of patients with PAH and may imply a lipotoxic cardiomyopathy in the RV in PAH.

possibly impaired right ventricle (RV) function in this PAH subtype. Germline mutations in *BMPR2*, a member of the transforming growth factor- β receptor family, are present in approximately 80% of heritable PAH. Despite a primarily pulmonary vascular phenotype of heritable PAH, mutant *BMPR2* is expressed throughout the affected individual, with potential for affecting organ structure and function outside the pulmonary circulation.

We and others have reported a high prevalence of metabolic derangements, including insulin resistance, dyslipidemia, and hyperglycemia, in both humans with PAH and in animal models of PAH (6–10). Recent work has highlighted a shift from glucose oxidation to glycolysis and accompanying impairment in fatty acid oxidation as a function of *BMPR2* mutation and in other animal models of PAH (11–13). With a high metabolic rate and preference for fatty acids as a fuel source, the heart may be particularly sensitive to

metabolic impairment as a function of *BMPR2* mutation. However, it is unknown if the presence of *BMPR2* mutation in the RV may alter responses of this organ to stressors such as increased afterload.

We hypothesized that expression of mutant *BMPR2* in the RV impairs hypertrophic responses in association with alterations in fatty acid oxidation. We tested this hypothesis in transgenic mouse models of *Bmpr2* mutation and in human heritable PAH RV tissue. Some of the results of these studies have been previously reported in the form of an abstract (14).

Methods

All animal procedures were approved by the Institutional Animal Care and Use Committee of Vanderbilt University School of Medicine, and human studies were approved by the Institutional Review Board of Vanderbilt University School of Medicine (IRB numbers 9401 and 111066).

Transgenic Mice

We used two models of mutant *Bmpr2* expression: (1) the Rosa26-rtTA2 \times TetO₇-*Bmpr2*^{R899X} FVB/N mice previously described (15, 16), called Rosa26^{R899X} for brevity (17), in which mutant *Bmpr2* is universally expressed; and (2) the Sm22-rtTA2 \times TetO₇-*Bmpr2*^{R899X},

called Sm22^{R899X} for brevity, in which mutant *Bmpr2* expression is confined to the smooth muscle (17). Expression of transgene occurs only after initiation of doxycycline in both models. Transgene-negative mice were used as littermate controls and were administered doxycycline as well.

In experiments using metformin, Rosa26^{R899X} mice were fed a high-fat chow (60% lard) with doxycycline and metformin (25 g/kg) or vehicle diet beginning at 6 weeks of age. Western diet has been shown to increase penetrance of PH in this model (18). This diet was continued for 6 weeks, at which time mice were killed as described below.

Pulmonary Artery Banding

Pulmonary artery banding (PAB) was performed as previously described (19) in FVB/N littermate control mice at 8 to 10 weeks of age at either low pressure (right ventricular systolic pressure [RVSP], 25–30 mm Hg) or high pressure (RVSP, 45–40 mm Hg) and remained in place for 2 weeks, after which animals underwent echocardiography, invasive hemodynamic measurement, and were killed, with tissue harvested and preserved in formalin or snap frozen. High-pressure PAB was also performed in Rosa26^{R899X} mice at 8 to 10 weeks of age after 2 weeks of doxycycline administration. PAB continued with

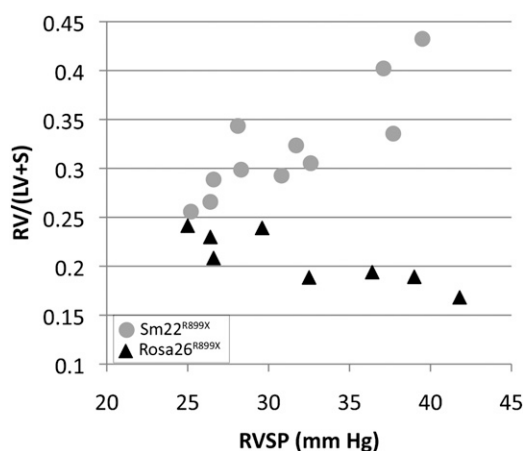


Figure 1. Right ventricular (RV) hypertrophy in smooth muscle-specific and universal expression of mutant *Bmpr2*. RV/(left ventricle + septum) ratio as a function of RV systolic pressure (RVSP) in two models of mutant *Bmpr2* expression: smooth muscle-specific, in which there is no RV expression of mutant *Bmpr2* (Sm22^{R899X}), and universal expression of mutant *Bmpr2* under the Rosa26 promoter (Rosa26^{R899X}), in which mutant *Bmpr2* is present in the RV. RV hypertrophy is absent as a function of RVSP in universal mutant *Bmpr2* expression, whereas it is preserved when mutant *Bmpr2* is confined to smooth muscle cells. Doxycycline was administered for 6 weeks in both models. $P < 0.01$ by analysis of covariance; $n = 8$ and 11, respectively.

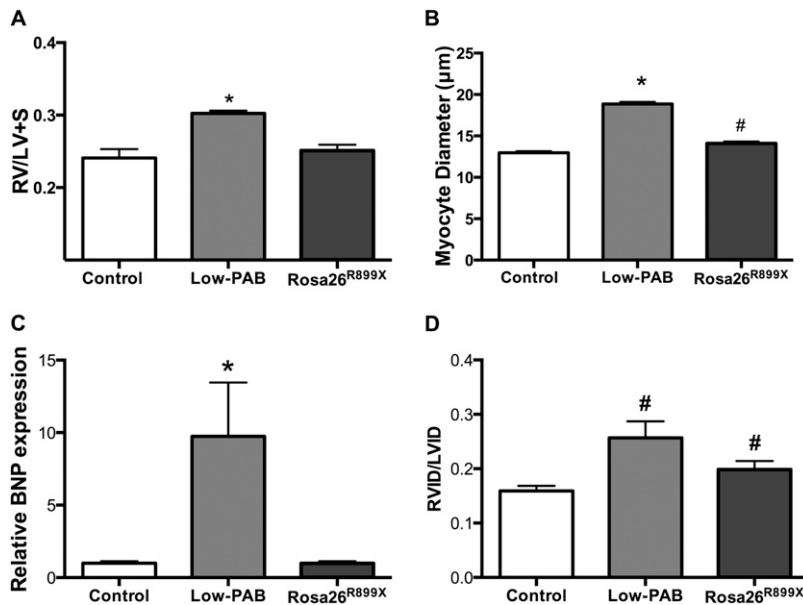


Figure 2. Right ventricular (RV) hypertrophy and dilation in control, low-pressure pulmonary artery banding (Low-PAB), and Rosa26^{R899X} mice. RV hypertrophic responses were compared in sham-treated control mice, littermate control mice that underwent Low-PAB, and Rosa26^{R899X} mice 6 weeks after transgene activation. (A) Macroscopic RV hypertrophy [RV/(left ventricle + septum)] in Rosa26^{R899X} is impaired compared with similar pressure by PAB (Low-PAB) in littermate control mice. $n = 5$ to 10 per group. (B) Myocyte diameter measurement on hematoxylin and eosin-stained RV tissue from the same groups showed decreased myocyte hypertrophy when mutant Bmpr2 is expressed in the RV compared with Low-PAB in littermate control mice, where myocyte diameter is substantially increased compared with control mice. $n = 3$ RVs, 75 to 100 myocytes per RV in three to four fields. (C) Relative brain natriuretic peptide (BNP) expression by quantitative polymerase chain reaction for the same groups demonstrated increased BNP expression in PAB that was not present in the similarly stressed Rosa26^{R899X} RVs. (D) RV dilation as measured by echocardiography is similar in Low-PAB and Rosa26^{R899X} mice, despite impaired hypertrophy in transgenic mice. RVID/LVID = right ventricular internal diameter/left ventricular internal diameter. $n = 6$ to 23 per group, * $P < 0.05$ versus control and Rosa26^{R899X}, # $P < 0.05$ versus control.

doxycycline for 2 weeks, when animals were killed as described above.

In Vivo Hemodynamics

At the time of sacrifice, invasive hemodynamics were measured either through a closed-chested technique for simple measurement of RVSP (17) or through open-chested technique for measurement of pressure–volume loops in animals after PAB, as in our hands this yields better quality pressure–volume loops (19). Both techniques have been previously described (17, 19). Hemodynamics were continuously recorded with a Millar MPVS-300 unit coupled to a Powerlab 8-SP analog-to-digital converter acquired at 1,000 Hz and captured to a Macintosh G4 (Millar Instruments, Houston, TX).

Histology

RVs were harvested at the time of sacrifice and snap frozen or placed in 10% formalin.

For oil red O staining, 10-μm frozen sections were cut and mounted on slides. Oil red O staining was performed as previously described (20). Further details can be found in the online supplement.

Expression Arrays

RNA was isolated from RVs using a Qiagen RNeasy mini kit (Valencia, CA). First and second strand complementary DNA was synthesized using standard techniques. Biotin-labeled antisense complementary RNA was produced by an *in vitro* transcription reaction. Human Gene 1.0 microarrays (Affymetrix, Foster City, CA) were hybridized with 20 μg cRNA. Target hybridization, washing, staining, and scanning probe arrays were done following an Affymetrix GeneChip Expression Analysis Manual. All array results have been submitted to the National Center for Biotechnology Information gene expression and hybridization array data repository

(GEO, <http://www.ncbi.nlm.nih.gov/geo/>) as series (pending). Arrays were analyzed as previously described (21).

Data Analysis

Statistical tests were either one-way or two-way analysis of variance (ANOVA) with *post hoc* Fisher least significant difference, or z-test, performed using the JMP program (SAS, Cary, NC) or GraphPad Prism Plus version 5.0 Software (San Diego, CA). Data are presented as mean \pm SD unless otherwise noted.

Results

Effects of Bmpr2 Mutation on RV Hypertrophy

To determine if expression of mutant Bmpr2 expression in the RV altered the expected hypertrophic responses in response to elevation in pulmonary artery pressure, we compared RV/(LV + S) (where LV is left ventricle and S is septum) ratio as a function of RV systolic pressure as measured by *in vivo* hemodynamics in two models of mutant Bmpr2 expression: (1) Rosa26^{R899X} with universal expression of mutant BMPR2 including the RV (16); and (2) Sm22^{R899X}, in which mutant expression is confined to smooth muscle and absent in cardiac myocytes (17) (Figure 1). In both transgenic models, doxycycline was administered for 6 weeks. We found that RV/(LV + S) directly correlated with RVSP in the Sm22^{R899X} mice. In contrast, in Rosa26^{R899X} mice with RV expression of mutant BMPR2, there was no increase in RV/(LV + S) in the context of increased pulmonary vascular pressures ($P < 0.01$ by analysis of covariance). We confirmed altered Bmpr2-related signaling in the Rosa26^{R899X} RVs compared with littermate control mice using immunostaining for both total and phospho-SMADs (see Figure E1 in the online supplement) and showed increased stain for both with expression of mutant Bmpr2 in the RV.

We next sought to compare RV hypertrophic responses in Rosa26^{R899X} mice with control mice and with a mouse model of RV hypertrophy (22–24), PAB, in wild-type controls (Figure 2A). We used low-pressure PAB (Low-PAB) with RVSP of approximately 25 to 30 mm Hg to mimic the load stress present in the Rosa26^{R899X} model. We found that on a macroscopic

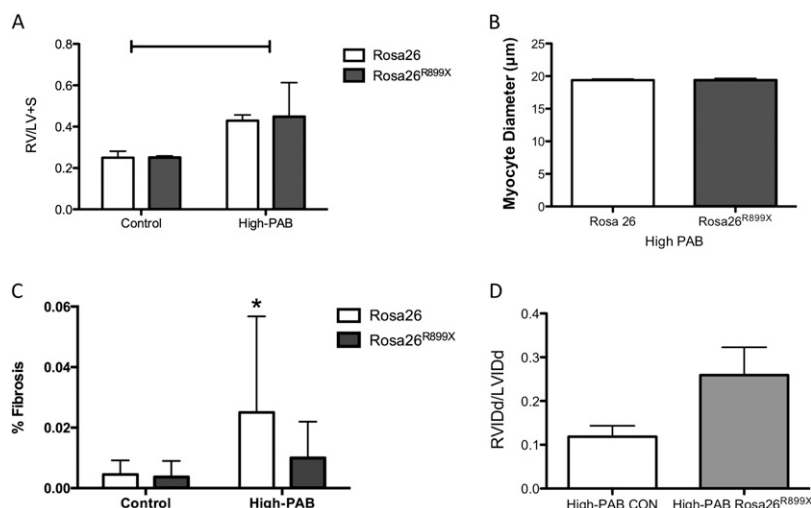


Figure 3. Effects of load stress on right ventricle (RV) hypertrophy and dilation in the context of *Bmpr2* mutation. RV hypertrophy was assessed in Rosa26^{R899X} mice that underwent high-pressure pulmonary artery banding (High-PAB) or sham 2 weeks after transgene activation and in littermate control mice. (A) RV/(LV + S) in control and High-PAB with mutant *Bmpr2* expression in the RV (Rosa26^{R899X}) and littermate control mice (Rosa26) demonstrating that with marked elevation in RV load stress, RV hypertrophy can be induced. The horizontal bar indicates $P < 0.05$ by two-way analysis of variance for effect of PAB. (B) Myocyte diameter was increased by PAB in both littermate control mice and Rosa26^{R899X} with High-PAB. (C) Percent fibrotic area was increased in Rosa26 RVs that underwent High-PAB but was not increased in the Rosa26^{R899X} RVs either at baseline or with High-PAB. * $P < 0.05$ versus control. (D) High-PAB in the context of *Bmpr2* mutation expression in the RV results in RV dilation, whereas hypertrophic response in High-PAB littermate controls results a nonsignificant trend toward less dilation, $P = 0.05$. $n = 4$ per group. LV = left ventricle; LVIDd = left ventricular internal diameter in diastole; RVIDd = right ventricular internal diameter in diastole; S = septum.

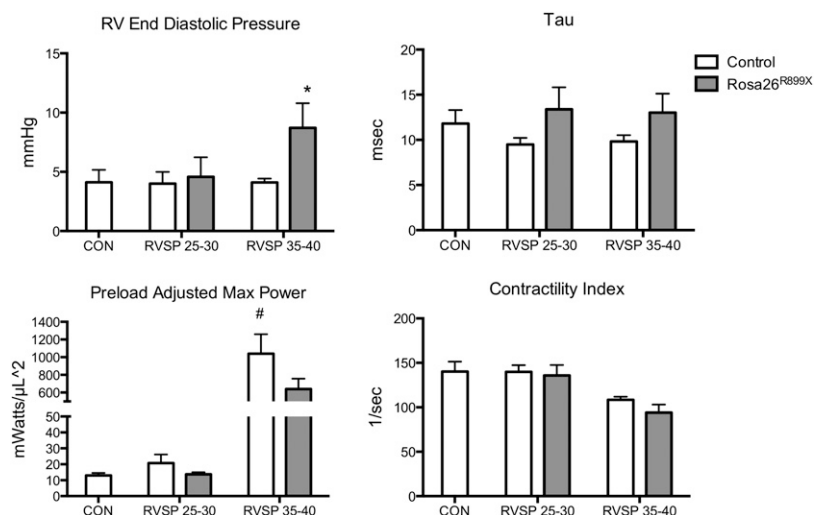


Figure 4. Hemodynamic effects of *Bmpr2* mutation in the right ventricle (RV) in both low-pressure (25–30 mm Hg) and high-pressure (35–40 mm Hg) pulmonary artery banding (PAB). *In vivo* hemodynamics were compared in three conditions: no load stress (CON), RV systolic pressure (RVSP) 25 to 30 mm Hg from either Low-PAB or transgene activation in the Rosa26^{R899X} model, and RVSP 35 to 40 mm Hg from High-PAB in littermate control mice or Rosa26^{R899X} mice that underwent High-PAB. Preload adjusted max power was increased by PAB at low (RVSP 25–30 mm Hg) and high (RVSP 35–40 mm Hg) pressure with a significant effect and interaction by the presence of mutant *Bmpr2* expression in the RV, # $P < 0.05$ by two-way analysis of variance for effect of PAB, transgene, and interaction of both. There was a drop in contractility index in both groups with PAB. RV end-diastolic pressure was substantially increased with high-PAB in transgenic animals (* $P < 0.05$) that was not found in littermate control mice. CON represents littermate control mice with no PAB. $n = 3$ to 7 per group.

level, there was significant RV hypertrophy as measured by RV/(LV + S) in Low-PAB mice ($P < 0.05$ vs. control). In contrast, despite similar levels of RV systolic pressure and thus afterload, there was no increase in RV hypertrophy in the Rosa26^{R899X} model. Examination of myocyte size in the three groups showed similar findings, with substantial increase in myocyte diameter in Low-PAB mice ($P < 0.05$ vs. sham control and vs. Rosa26^{R899X}). Myocyte diameter was not statistically different in Rosa26^{R899X} mice from control mice (Figure 2B). We also measured expression of brain natriuretic peptide (BNP) by reverse transcriptase-polymerase chain reaction (PCR) as a marker of hypertrophic stimulus and found that although Low-PAB caused an expected increase in BNP expression, despite similar pressure, BNP expression was not increased in the Rosa26^{R899X} RVs ($P < 0.05$ vs. PAB; Figure 2C). Using M-mode echocardiography we measured RV dilation in control, Low-PAB wild-type, and Rosa26^{R899X} mice and found that the RV was significantly dilated in the Low-PAB mice and the Rosa26^{R899X} mice compared with control mice ($P < 0.05$; Figure 2D), demonstrating that load stress was present in both experimental models. These data show impaired RV macroscopic and cellular hypertrophic responses with mutant *BMPR2* expression in the RV.

To determine if the RV is capable of hypertrophy with a more significant load stress when mutant *Bmpr2* is expressed in the RV, we used standard pressure PAB (RVSP, approximately 40 mm Hg) in Rosa26 littermate control mice and Rosa26^{R899X} transgenic animals (Figure 3). For these experiments, PAB was performed at 8 to 10 weeks of age and animals killed 2 weeks later. Rosa26^{R899X} mice were treated with doxycycline continuously starting 2 weeks before PAB. We found similar RV/(LV + S) with high-pressure PAB in both littermate control mice and transgenic animals ($P < 0.05$ for effect of PAB by two-way ANOVA; Figure 3A). Myocyte diameter findings were similar (Figure 3B). In littermate control mice, PAB was associated with an increase in percent of RV fibrosis on Masson's trichrome stain; less fibrosis was observed in the Rosa26^{R899X} RVs, and it was not different from control mice (Figure 3C). On echocardiography, there was a trend to increased RV diameter in the PAB

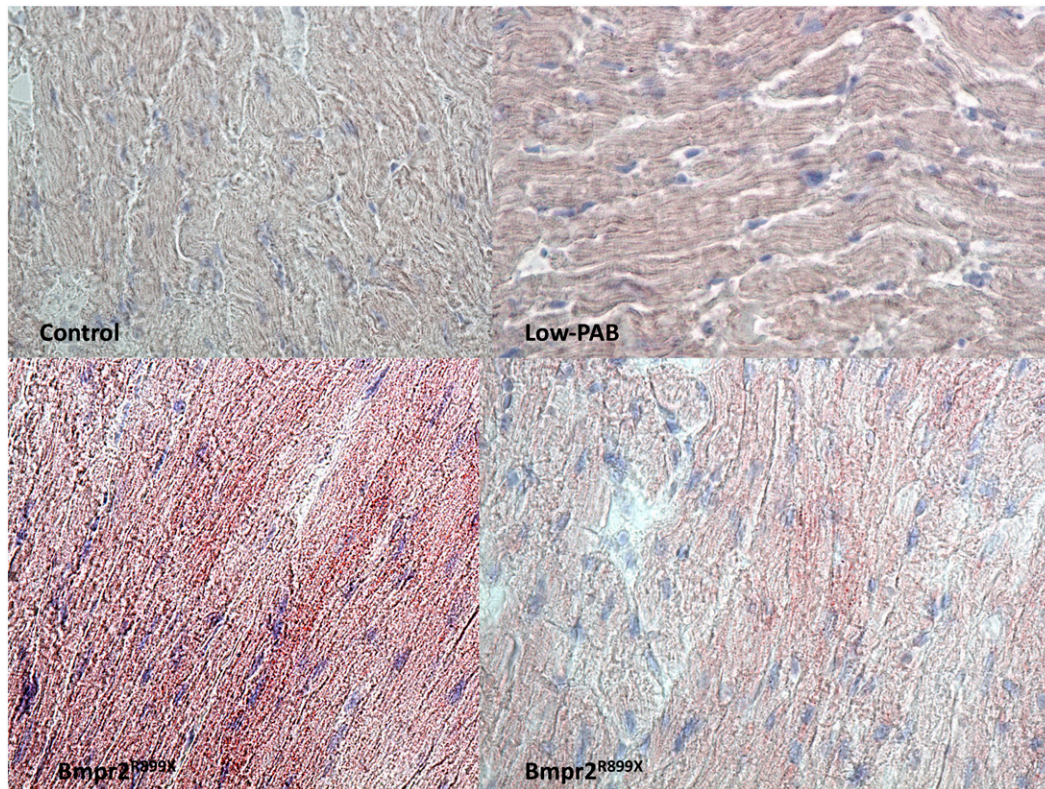


Figure 5. Oil red O staining in the right ventricle (RV) with and without *Bmpr2* mutation expression. Demonstration of lipid accumulation in the RVs of two *Rosa26^{R899X}* mice in which mutant *Bmpr2* is expressed in the RV (bottom two panels). Transgene was activated for 6 weeks. Both littermate control (upper left) and littermate control with low pulmonary artery banding (PAB) (upper right) did not demonstrate lipid droplets. Lipid in transgenic animals is demonstrated within cardiomyocytes. Lipid shown as red staining. 40× magnification shown.

Rosa26^{R899X} mice compared with PAB littermate control mice that was not statistically significant ($P = 0.05$; Figure 3D). These data suggest that RVs with mutant *Bmpr2* are capable of hypertrophy but in the context of severe load stress.

In Vivo Hemodynamic Effects of *Bmpr2* Mutation in the RV

We next sought to determine if alterations in hypertrophic responses with mutant *Bmpr2* expression in the RV would be accompanied by impaired hemodynamic compensation. We measured open-chested *in vivo* hemodynamics in three groups: littermate control mice with (1) sham PAB (control), (2) Low-PAB with RVSP 25 to 30 mm Hg, and (3) High-PAB with RVSP 35 to 40 mm Hg. We also measured *in vivo* hemodynamics in *Rosa26^{R899X}* mice under the same Low- and High-PAB conditions with transgene induction continuously beginning 2 weeks before PAB (Figure 4). We analyzed pressure–volume loops in each condition and found a significant increase in RV end-diastolic pressure ($P <$

0.05 by two-way ANOVA) in mice with RV expression of mutant *Bmpr2* (*Rosa26^{R899X}*). Preload adjusted maximum power was increased by PAB in all groups, but two-way ANOVA analysis demonstrated a decrease in transgenic animals compared with littermate control mice that was significant ($P < 0.05$). Overall, these data suggested depressed diastolic and systolic compensation in the context of load stress with mutant *Bmpr2* expression in the RV.

Lipid Deposition in the RV of *Rosa26^{R899X}* Mice

We have recently shown that abnormalities in fatty acid oxidation are associated with *BMPR2* mutation in pulmonary microvascular endothelial cells (11). Because the heart preferentially oxidizes fatty acids as a fuel source, we hypothesized that defects in fatty acid oxidation may result in accumulation of lipid in the RV of mice with RV expression of mutant *Bmpr2*. We tested this hypothesis by performing oil red O stains in littermate control and High-PAB mice and in *Rosa26^{R899X}* mice

after 6 weeks of transgene activation (Figure 5; digitally enhanced version can be found in Figure E2). We did not find evidence of significant lipid in normal RVSP littermate control mice or load-stressed littermate control mice (shown as Low-PAB in Figure 5). However, in the *Rosa26^{R899X}* mice, there was accumulation of lipid within the cardiomyocyte, with no lipid deposition in the extracellular space. *Rosa26^{R899X}* mice with normal RVSP demonstrated lipid deposition as well (Figure E2). There was little lipid accumulation in the left ventricle of the *Rosa26^{R899X}* mice (Figure E3); however, lipid deposition did not require increased afterload, as even mice with normal RVSP did have some evidence of lipid deposition (Figure E2). This qualitative increase in RV lipid was confirmed by mass spectrometry–measured total lipid content ($P < 0.05$; Figure 6). To determine the specific lipid present within the RV of the transgenic animals compared with littermate control mice, lipid extraction and thin-layer chromatography were

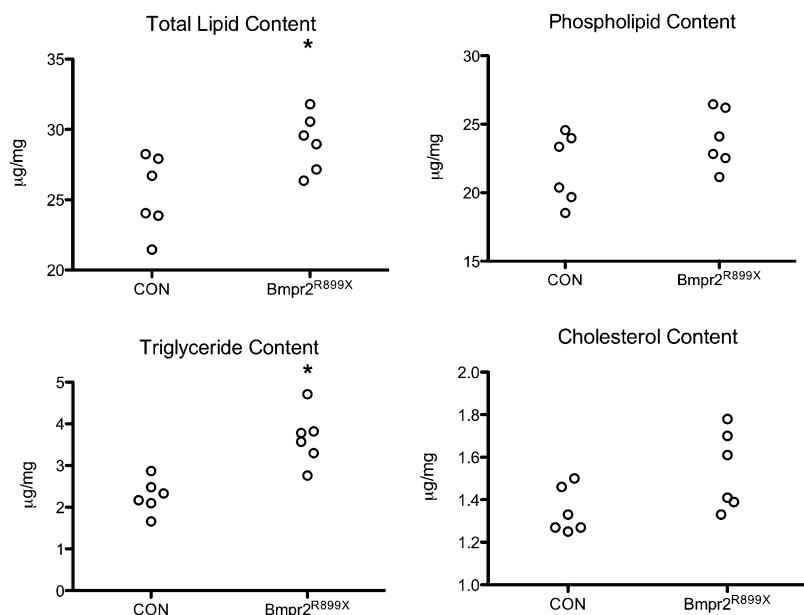


Figure 6. Total lipid, phospholipid, triglyceride, and cholesterol content in right ventricles (RVs) of mice with mutant *Bmpr2* expression in the RV and littermate control mice (CON). Transgene was activated for 6 weeks. Mass spectroscopy-measured total lipid content was significantly increased (* $P < 0.05$). Further analysis demonstrated that the intracellular lipid, triglyceride, was significantly increased in *Rosa26^{R899X}* mice compared with control mice ($P < 0.05$). Membrane phospholipid was not different in the two groups. $n = 6$ per group.

performed (Figure 6). There was no increase in membrane phospholipid content, but there was a significant increase in triglyceride content ($P < 0.05$) in the transgenic RVs with expression of mutant *Bmpr2*. We measured plasma lipids in the littermate control and *Rosa26^{R899X}* mice and found no difference in quantity or type of circulating lipids in the two groups (Figure E5). These data show increased intracardiomyocyte lipid, specifically triglyceride, in the RV when mutant *BMPR2* is expressed.

To explore whether potentially lipotoxic lipids are expressed in the RV with mutant *Bmpr2* expression, we tested the hypothesis that ceramide, a mediator of cardiac apoptosis and lipotoxicity (25–27), was increased in the *Rosa26^{R899X}* RV compared with control mice (Figure 7). First we performed immunohistochemistry for serine palmitoyltransferase 1 (SPT1), a key enzyme in the synthesis of ceramide (Figure 7) (28). We found patchy distribution and increased SPT1 staining both qualitatively and semiquantitatively, suggesting increased ceramide synthesis in the *Rosa26^{R899X}* RV. We also performed immunohistochemistry analysis of the same tissue for ceramide and found increased RV ceramide. As diacylglycerol has also

been implicated in mediating cardiac lipotoxicity (29), we performed an assay to measure RV diacylglycerol levels and did not find any difference between *Rosa26^{R899X}* mice and littermate control mice (Figure E6).

Metabolic Effects of Mutant *BMPR2* Expression in the Human RV

We first confirmed that *BMPR2* is expressed in the human RV using quantitative PCR in three human control RVs and two RVs obtained from patients with heritable PAH at autopsy (Figure E7). Levels of expression were similar to those obtained from human lung. To determine if alterations of lipid metabolism found in our transgenic mice are present in RV samples from human patients with heritable PAH and are distinct from normal RV metabolism and other forms of right heart failure, we obtained samples of RV tissue from healthy control subjects and from patients with idiopathic dilated cardiomyopathy (DCM) (Vanderbilt Heart and Vascular Institute Main Heart Registry, $n = 2$ each) and isolated RNA from these groups as well as our heritable PAH RVs ($n = 2$). Gene expression analysis of these RVs was performed using Affymetrix Gene 1.0 chips. From 28,763 initial probe sets, 9,837 have

both a median expression over 7 and a range of over 0.4 in log base 2 units. Restricting analysis to these genes prevents inclusion of noise. Undirected principal components analysis using all 9,837 probe sets identified a principal component that accounted for 31% of the total variability in the samples, which correctly divided the samples into three groups (the eigenvalues for healthy control subjects averaged -0.51 , for DCM 0.05 , and for PAH 0.46). The list of probes associated with this principal component was very similar to a list generated by ranking probes by fold change of PAH compared with healthy control subjects. Hierarchical clustering was performed using the top 200 genes from this list (using algorithms internal to dChip) and the genes in the branches individually examined for statistically overrepresented biological process ontology groups using Webgestalt (Figure 8A). These include up-regulation of several developmental pathways (Figure 8B), with DCM samples intermediate between PAH and healthy control subjects.

Presented in Figure 8A is statistical overrepresentation determined branch by branch. When analyzed as a group, the domination of metabolic pathways becomes even more striking. There are 430 unique genes differentially regulated at least two times in heritable PAH compared with healthy control subjects. Of these, 244 are metabolic (statistically overrepresented at $P = 0.0048$). We have recently published data indicating that *BMPR2* mutation in pulmonary microvascular endothelium is associated with a suppression of tricarboxylic acid cycle and lipid oxidation and an induction of glycolysis (11). Examination of the metabolic changes in PAH hearts suggests that the same defects are present in these samples (Figures 8C and 8D, for examples). Confirmatory PCR of selected fatty acid oxidation genes is shown in Figure E8.

Lipid Deposition in the RV of Patients with Human Heritable PAH

Using frozen sections from the idiopathic DCM control RV and heritable PAH RVs described above, we performed oil red O staining to determine if lipid deposition is present in humans with heritable PAH. We found extensive lipid deposition within cardiomyocytes of both human heritable PAH RVs (Figure 9). As in the mouse

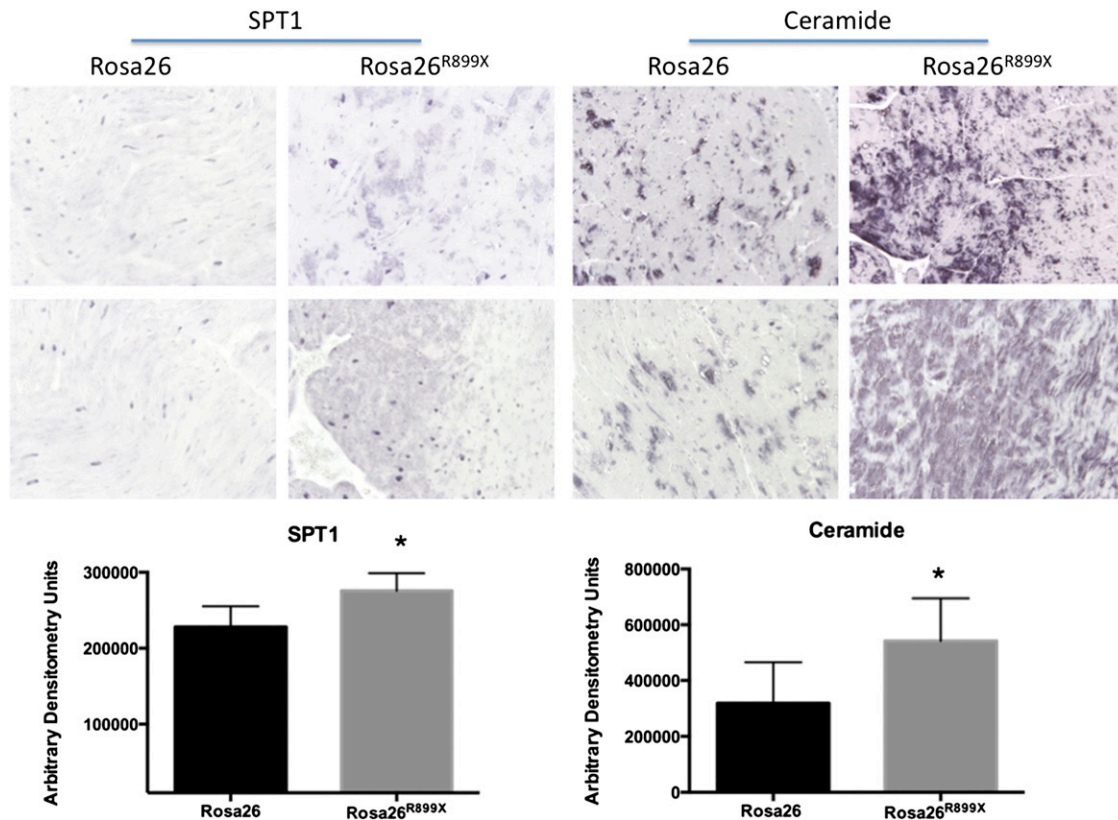


Figure 7. Serine palmitoyltransferase 1 (SPT1) and ceramide expression in the right ventricle (RV). We performed immunohistochemistry for SPT1 in the RV of Rosa26^{R899X} mice and littermate control mice, and data were analyzed qualitatively and semiquantitatively using photometric analysis. We found evidence of increased SPT1 and ceramide in the Rosa26^{R899X} RV compared with littermate control mice (* $P < 0.05$).

model, there was no significant lipid deposition extracellularly in the human RVs. There was minimal lipid deposition in human disease control RVs.

Prevention of Lipid Deposition with Metformin Administration

To test the hypothesis that drug therapy to enhance fatty acid oxidation prevents lipid deposition in the RV in Rosa26^{R899X} mice, we administered metformin or vehicle to Rosa26^{R899X} mice (Figure 10). By oil red O stain we found markedly decreased RV lipid deposition both qualitatively (Figures 10A and 10B) and quantitatively (Figure 10C; $P < 0.05$).

Discussion

In these experiments we have used transgenic mouse models with and without RV expression of mutant Bmpr2 as well as PAB, an RV hypertrophy model, to demonstrate that mutant Bmpr2 expression in the RV is associated with impaired RV

hypertrophic responses and decreased hemodynamic compensation for load stress. We further demonstrated increased lipid content, specifically intracellular triglyceride, in RVs with mutant Bmpr2 expression, and we have shown that this does not appear to be a general response to RV load stress. Furthermore, we have found evidence for increased synthesis and deposition of ceramide, which has been shown to be lipotoxic (25, 28). We have extended these findings to human heritable PAH RVs, where we found alteration in expression of genes associated with fatty acid oxidation and lipid deposition, and we have demonstrated in mice that RV lipid deposition is reversible using metformin. In summary, these data suggest that mutant *BMPR2* expression in the RV may impair hypertrophic responses in part due to fatty acid oxidation defects.

The *BMPR2* receptor is a member of the transforming growth factor- β receptor family, signaling through which has recently been linked to the development

of maladaptive left ventricular hypertrophy (30). The role of Bmpr2 signaling in mediating RV load stress responses including hypertrophy has not been explored but has biologic relevance given the universal expression of this mutation in some human forms of PAH. Our Rosa26^{R899X} data suggest that impaired cardiomyocyte *BMPR2* signaling via receptor cytoplasmic domain mutation limits the ability of the RV to hypertrophy in response to increased pressure.

In addition to potential effects of dysfunctional Bmpr2 signaling in limiting cardiac hypertrophy, Bmpr2 dysfunction has been linked by our group and others to metabolic alterations. In particular, defective peroxisome proliferator-activated receptor- γ signaling resulting has been reported as a function of Bmpr2 mutation (7, 8) as well as increased glycolysis, decreased oxidative phosphorylation, and impairment in fatty acid oxidation (11). Impairments in lipid metabolism and insulin resistance are closely associated with tissue lipid deposition (29, 31, 32).

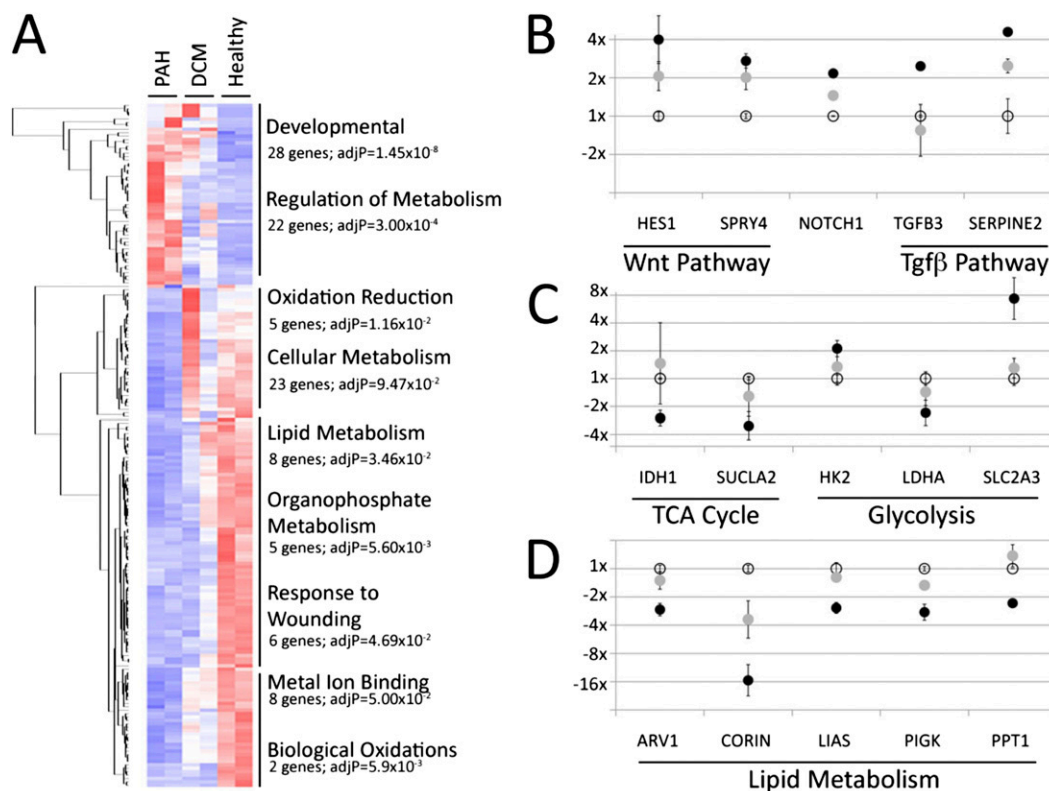


Figure 8. Gene expression analysis of biopsies of human right ventricles from patients with pulmonary arterial hypertension (PAH) or dilated cardiomyopathy (DCM) or healthy control subjects. (A) Hierarchical clustering of genes differentially regulated in subjects with PAH compared with healthy control subjects shows that the differences are dominated by genes related to metabolism, with some stress and developmental genes in addition. DCM samples showed an intermediate expression profile between subjects with PAH and healthy control subjects. (B) Developmental pathways altered included an up-regulation in Wnt, Notch, and Tgfb pathways. For B–D, open circles represent the average of healthy control subjects; gray circles, DCM; and black circles PAH. Error bars are SEM. (C) Metabolic gene expression changes suggested a suppression of tricarboxylic acid cycle and an increase in glycolysis. (D) Gene expression changes also suggest a decrease in derivation of energy from lipid metabolism. $n = 2$ samples per condition. TGF = transforming growth factor.

Animal models have demonstrated that lipid deposition in the myocardium, even without insulin resistance, leads to left ventricular cardiomyopathy (33, 34). Our findings of potential lipotoxic effects as shown by hemodynamics and ceramide data in the RV associated with *Bmpr2* mutation are new. Our finding of lipid deposition even without pulmonary hypertension in the Rosa26^{R899X} model and absent lipid with PAB in littermate control mice suggest that RV lipotoxicity is unlikely just due to increased afterload. The extension of these mouse findings in human RV samples suggests that there may be RV-specific effects of *BMPR2* mutation in humans.

Moreover, impairment in fatty acid oxidation pathways may also underlie the observed limitation in cardiac hypertrophy, as fatty acid oxidation is the preferred energy source in the cardiomyocyte (35). With impairment in fatty acid oxidation, there will be decreased substrate availability

for catabolism, increased use of glucose through Randle's cycle, and thus an abnormal energy use pattern in the RV (35). Recent work by other groups has highlighted the critical role of fatty acid oxidation in rodent models of RV stress responses. RV dysfunction correlates with decreased expression of intermediaries of fatty acid oxidation and RV hypertrophy with increased intermediaries of fatty acid oxidation (23, 24). Our data corroborate these findings in that reduced expression of fatty acid oxidation genes was present in human failing RV samples, and when a transgenic model of *Bmpr2* mutation resulting in impaired fatty acid oxidation was used, hypertrophy was inhibited. We used metformin to enhance fatty acid oxidation and found reduced lipid deposition, suggesting that lipotoxicity may be reversible and a potential therapeutic target. These data highlight the role of RV energy substrate use in determining failure

or hypertrophic phenotype and suggest that this may be a future therapeutic target.

Prior studies of RV dysfunction in animal models have been unclear in extrapolation to human disease. A transgenic model of RV dysfunction that uses overexpression of a human mutation may be a useful and clinically applicable model for future studies of mechanisms of human RV failure and trials of RV-directed therapeutics in PAH. Studies of drug therapy to alter impaired energy metabolism in the RV may be particularly informative in this model.

Our study does have some limitations. Other mechanisms that drive lipid deposition, such as lipid synthesis and transport, how insulin resistance affects cardiomyocyte signaling, and how glucose import and metabolism are affected by *Bmpr2* mutation, are not addressed by these studies, and will be areas of future study. We have attempted to demonstrate lipid

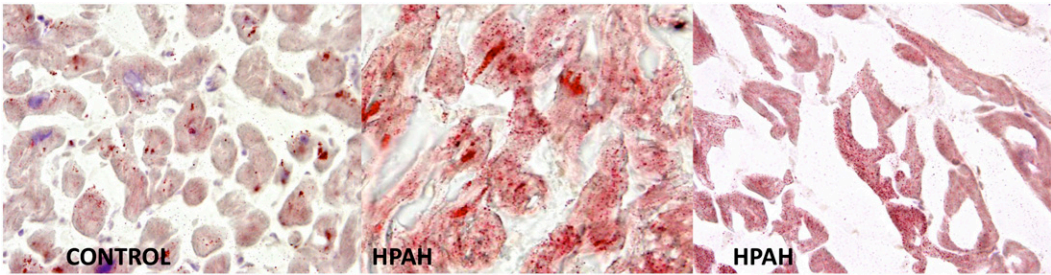


Figure 9. Oil red O staining in human idiopathic dilated cardiomyopathy right ventricle (RV) and two human heritable pulmonary arterial hypertension (HPAH) RVs. Striking lipid staining is present in the heritable PAH RVs that is greatly enhanced compared with the idiopathic dilated cardiomyopathy sample.

deposition is not related to afterload stress, but there may be a pulmonary vascular effect of metformin that affects RV stress responses and will require more study in the future. Finally, our findings will require exploration in other animal models and other types of human RV failure.

In conclusion, we have demonstrated impaired RV hypertrophy, hemodynamic

compensation associated with triglyceride deposition in a model of mutant *Bmpr2* expression in the RV. We have correlated these findings with human RVs from patients with heritable PAH and demonstrated lipid deposition and alteration in fatty acid oxidation. Further study of the role of underlying mechanisms of BMPR2 in mediating RV hypertrophy

and cardiac energy metabolism is warranted. ■

Author disclosures are available with the text of this article at www.atsjournals.org.

Acknowledgment: The authors thank the Vanderbilt Heart and Vascular Institute's Main Heart Registry for use of human RV tissue and Yan Ru Su, MD, for help with tissue acquisition and preparation.

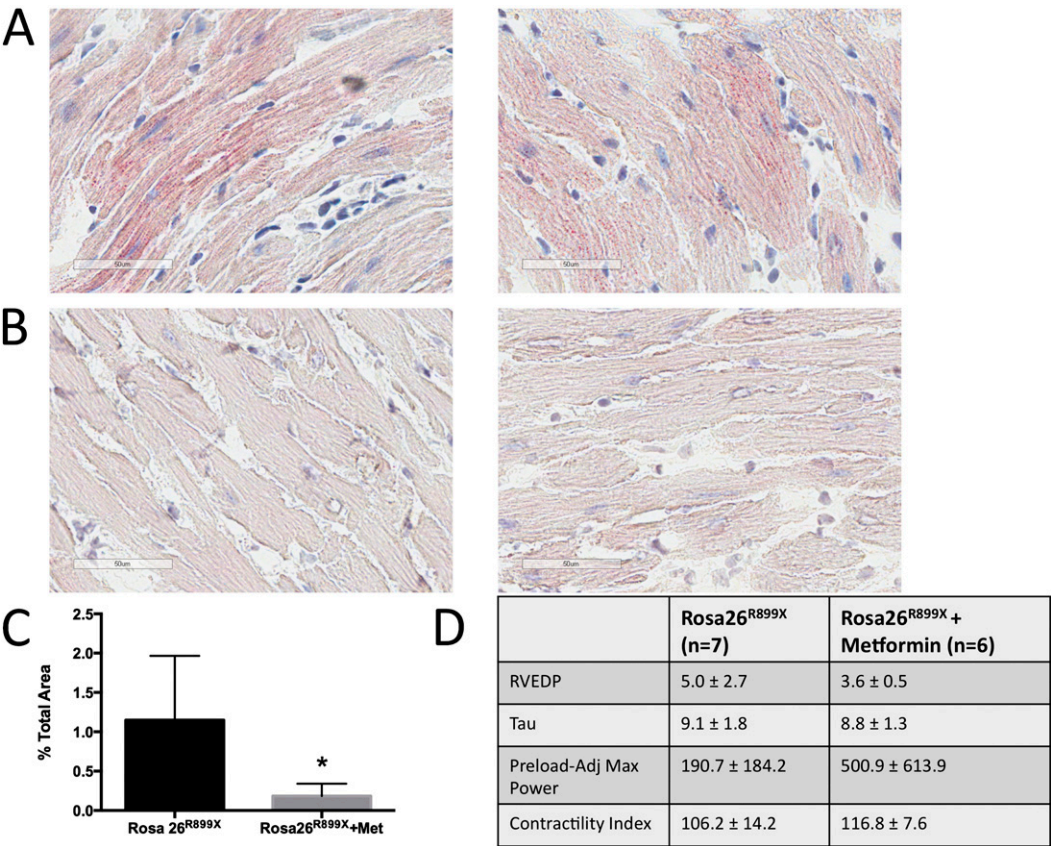


Figure 10. Effects of metformin on right ventricle (RV) lipid deposition in Rosa26^{R899X} mice and vehicle-fed control mice. Rosa26^{R899X} mice were fed a Western diet with doxycycline with or without metformin for 6 weeks. Extensive lipid deposition was demonstrated in the RV in Rosa26^{R899X} mice (A); however, metformin substantially decreased lipid deposition (B and C, **P* < 0.05 vs. Rosa26; *n* = 8–10 per group). In C, images are converted as demonstrated in Figure E2, and moderate to strong red staining is quantified as percent of total area. Table in D includes results from *in vivo* hemodynamic measurements. No comparisons are statistically significant. Met = metformin; RVEDP = right ventricular end diastolic pressure.

References

- Voelkel NF, Quaife RA, Leinwand LA, Barst RJ, McGoon MD, Meldrum DR, Dupuis J, Long CS, Rubin LJ, Smart FW, *et al.*: National Heart, Lung, and Blood Institute Working Group on Cellular and Molecular Mechanisms of Right Heart Failure. Right ventricular function and failure: report of a National Heart, Lung, and Blood Institute working group on cellular and molecular mechanisms of right heart failure. *Circulation* 2006;114:1883–1891.
- Humbert M, Sitbon O, Chaouat A, Bertocchi M, Habib G, Gressin V, Yaïci A, Weitzenblum E, Cordier JF, Chabot F, *et al.* Survival in patients with idiopathic, familial, and anorexigen-associated pulmonary arterial hypertension in the modern management era. *Circulation* 2010;122:156–163.
- Benza RL, Miller DP, Gomberg-Maitland M, Frantz RP, Foreman AJ, Coffey CS, Frost A, Barst RJ, Badesch DB, Elliott CG, *et al.* Predicting survival in pulmonary arterial hypertension: insights from the Registry to Evaluate Early and Long-term Pulmonary Arterial Hypertension Disease Management (REVEAL). *Circulation* 2010;122:164–172.
- Girerd B, Montani D, Eyries M, Yaïci A, Sztrymf B, Coulet F, Sitbon O, Simonneau G, Soubrier F, Humbert M. Absence of influence of gender and BMPR2 mutation type on clinical phenotypes of pulmonary arterial hypertension. *Respir Res* 2010;11:73.
- Brittain E, Pugh ME WL, Robbins IM, Loyd JE, Newman JH, Larkin EK, Austin ED, Hemnes AR. Shorter survival in hereditary versus idiopathic pulmonary arterial hypertension is associated with hemodynamic markers of impaired in right ventricular function. *Pulm Circ* (In press)
- Zamanian RT, Hansmann G, Snook S, Lilienfeld D, Rappaport KM, Reaven GM, Rabinovitch M, Doyle RL. Insulin resistance in pulmonary arterial hypertension. *Eur Respir J* 2009;33:318–324.
- Hansmann G, de Jesus Perez VA, Alastalo TP, Alvira CM, Guignabert C, Bekker JM, Schellong S, Urashima T, Wang L, Morrell NW, *et al.* An antiproliferative BMP-2/PPARgamma/apoE axis in human and murine SMCs and its role in pulmonary hypertension. *J Clin Invest* 2008;118:1846–1857.
- Hansmann G, Wagner RA, Schellong S, Perez VA, Urashima T, Wang L, Sheikh AY, Suen RS, Stewart DJ, Rabinovitch M. Pulmonary arterial hypertension is linked to insulin resistance and reversed by peroxisome proliferator-activated receptor-gamma activation. *Circulation* 2007;115:1275–1284.
- Pugh ME, Robbins IM, Rice TW, West J, Newman JH, Hemnes AR. Unrecognized glucose intolerance is common in pulmonary arterial hypertension. *J Heart Lung Transplant* 2011;30:904–911.
- Heresi GA, Aytikin M, Newman J, DiDonato J, Dweik RA. Plasma levels of high-density lipoprotein cholesterol and outcomes in pulmonary arterial hypertension. *Am J Respir Crit Care Med* 2010;182:661–668.
- Fessel JP, Hamid R, Wittmann BM, Robinson LJ, Blackwell T, Tada Y, Tanabe N, Tatsumi K, Hemnes AR, West JD. Metabolic analysis of bone morphogenetic protein receptor type 2 mutations in human pulmonary endothelium reveals widespread metabolic reprogramming. *Pulm Circ* 2012;2:201–213.
- Piao L, Fang YH, Cadete VJ, Wietholt C, Urboniene D, Toth PT, Marsboom G, Zhang HJ, Haber I, Rehman J, *et al.* The inhibition of pyruvate dehydrogenase kinase improves impaired cardiac function and electrical remodeling in two models of right ventricular hypertrophy: resuscitating the hibernating right ventricle. *J Mol Med (Berl)* 2010;88:47–60.
- Sutendra G, Bonnet S, Rochefort G, Haromy A, Folmes KD, Lopaschuk GD, Dyck JR, Michelakis ED. Fatty acid oxidation and malonyl-CoA decarboxylase in the vascular remodeling of pulmonary hypertension. *Sci Transl Med* 2010;2:44ra58.
- Hemnes AR, Fessel JP, Penner N, Gleaves L, Robinson L, West J. Universal expression of BMPR2 mutation is associated with impairment of right ventricular hypertrophy and steatosis in mice [abstract]. *Am J Respir Crit Care Med* 2012;185:A3454.
- Yasuda T, Tada Y, Tanabe N, Tatsumi K, West J. Rho-kinase inhibition alleviates pulmonary hypertension in transgenic mice expressing a dominant-negative type II bone morphogenetic protein receptor gene. *Am J Physiol Lung Cell Mol Physiol* 2011;301:L667–L674.
- Johnson JA, Hemnes AR, Perrien DS, Schuster M, Robinson LJ, Gladson S, Loibner H, Bai S, Blackwell TR, Tada Y, *et al.* Cytoskeletal defects in Bmpr2-associated pulmonary arterial hypertension. *Am J Physiol Lung Cell Mol Physiol* 2012;302:L474–L484.
- West J, Harral J, Lane K, Deng Y, Ickes B, Crona D, Albu S, Stewart D, Fagan K. Mice expressing BMPR2R899X transgene in smooth muscle develop pulmonary vascular lesions. *Am J Physiol Lung Cell Mol Physiol* 2008;295:L744–L755.
- West J, Niswender KD, Johnson JA, Pugh ME, Gleaves L, Fessel JP, Hemnes AR. A potential role for insulin resistance in experimental pulmonary hypertension. *Eur Respir J* 2013;41:861–871.
- Johnson JA, West J, Maynard KB, Hemnes AR. ACE2 improves right ventricular function in a pressure overload model. *PLoS ONE* 2011;6:e20828.
- Postic C, Shiota M, Niswender KD, Jetton TL, Chen Y, Moates JM, Shelton KD, Lindner J, Cherrington AD, Magnuson MA. Dual roles for glucokinase in glucose homeostasis as determined by liver and pancreatic beta cell-specific gene knock-outs using Cre recombinase. *J Biol Chem* 1999;274:305–315.
- Austin ED, Menon S, Hemnes AR, Robinson LR, Talati M, Fox KL, Cogan JD, Hamid R, Hedges LK, Robbins I, *et al.* Idiopathic and heritable PAH perturb common molecular pathways, correlated with increased MSX1 expression. *Pulm Circ* 2011;1:389–398.
- Bogaard HJ, Natarajan R, Henderson SC, Long CS, Kraskauskas D, Smithson L, Ockaili R, McCord JM, Voelkel NF. Chronic pulmonary artery pressure elevation is insufficient to explain right heart failure. *Circulation* 2009;120:1951–1960.
- Gomez-Arroyo J, Mizuno S, Szczepanek K, Van Tassel B, Natarajan R, dos Remedios CG, Drake JI, Farkas L, Kraskauskas D, Wijesinghe DS, *et al.* Metabolic gene remodeling and mitochondrial dysfunction in failing right ventricular hypertrophy secondary to pulmonary arterial hypertension. *Circ Heart Fail* 2013;6:136–144.
- Fang YH, Piao L, Hong Z, Toth PT, Marsboom G, Bache-Wiig P, Rehman J, Archer SL. Therapeutic inhibition of fatty acid oxidation in right ventricular hypertrophy: exploiting Randle's cycle. *J Mol Med (Berl)* 2012;90:31–43.
- Baranowski M, Górski J. Heart sphingolipids in health and disease. *Adv Exp Med Biol* 2011;721:41–56.
- Sharma S, Adroge JV, Golfman L, Uray I, Lemm J, Youker K, Noon GP, Frazier OH, Taegtmeyer H. Intramyocardial lipid accumulation in the failing human heart resembles the lipotoxic rat heart. *FASEB J* 2004;18:1692–1700.
- Wende AR, Abel ED. Lipotoxicity in the heart. *Biochim Biophys Acta* 2010;1801:311–319.
- Ussher JR, Folmes CD, Keung W, Fillmore N, Jaswal JS, Cadete VJ, Beker DL, Lam VH, Zhang L, Lopaschuk GD. Inhibition of serine palmitoyl transferase I reduces ceramide levels and increases glycolysis rates following diet-induced insulin resistance. *PLoS ONE* 2012;7:e37703.
- Samuel VT, Petersen KF, Shulman GI. Lipid-induced insulin resistance: unravelling the mechanism. *Lancet* 2010;375:2267–2277.
- Koibabashi N, Danner T, Zaiman AL, Pinto YM, Rowell J, Mankowski J, Zhang D, Nakamura T, Takimoto E, Kass DA. Pivotal role of cardiomyocyte TGF- β signaling in the murine pathological response to sustained pressure overload. *J Clin Invest* 2011;121:2301–2312.
- Morino K, Petersen KF, Sono S, Choi CS, Samuel VT, Lin A, Gallo A, Zhao H, Kashiwagi A, Goldberg IJ, *et al.* Regulation of mitochondrial biogenesis by lipoprotein lipase in muscle of insulin-resistant offspring of parents with type 2 diabetes. *Diabetes* 2012;61:877–887.
- Samuel VT, Shulman GI. Mechanisms for insulin resistance: common threads and missing links. *Cell* 2012;148:852–871.
- Duncan JG, Bharadwaj KG, Fong JL, Mitra R, Sambandam N, Courtois MR, Lavine KJ, Goldberg IJ, Kelly DP. Rescue of cardiomyopathy in peroxisome proliferator-activated receptor- α transgenic mice by deletion of lipoprotein lipase identifies sources of cardiac lipids and peroxisome proliferator-activated receptor- α activators. *Circulation* 2010;121:426–435.
- Glenn DJ, Wang F, Nishimoto M, Cruz MC, Uchida Y, Holleran WM, Zhang Y, Yeghiazarians Y, Gardner DG. A murine model of isolated cardiac steatosis leads to cardiomyopathy. *Hypertension* 2011;57:216–222.
- Lopaschuk GD, Ussher JR, Folmes CD, Jaswal JS, Stanley WC. Myocardial fatty acid metabolism in health and disease. *Physiol Rev* 2010;90:207–258.